Acta Biomaterialia 118 (2020) 153–160

Contents lists available at ScienceDirect

Acta Biomaterialia

journal homepage: www.elsevier.com/locate/actbio

Collagen denaturation is initiated upon tissue yield in both positional and energy-storing tendons ☆

Allen H. Lin[a,b], Alexandra N. Allan[a,b], Jared L. Zitnay[a,b], Julian L. Kessler[a], S. Michael Yu[a,c], Jeffrey A. Weiss[a,b,d,*]

[a] Department of Biomedical Engineering, University of Utah, United States
[b] Scientific Computing and Imaging Institute, University of Utah, United States
[c] Department of Pharmaceutics and Pharmaceutical Chemistry, University of Utah, United States
[d] Department of Orthopaedics, University of Utah, United States

ARTICLE INFO

Article history:
Received 11 June 2020
Revised 4 September 2020
Accepted 30 September 2020
Available online 6 October 2020

Keywords:
Denatured collagen
Energy-storing tendon
Positional tendon
Collagen hybridizing peptide
Tendon failure

ABSTRACT

Tendons are collagenous soft tissues that transmit loads between muscles and bones. Depending on their anatomical function, tendons are classified as positional or energy-storing with differing biomechanical and biochemical properties. We recently demonstrated that during monotonic stretch of positional tendons, permanent denatured collagen begins accumulating upon departing the linear region of the stress-strain curve. However, it is unknown if this observation is true during mechanical overload of other types of tendons. Therefore, the purpose of this study was to investigate the onset of collagen denaturation relative to applied strain, and whether it differs between the two tendon types. Rat tail tendon (RTT) fascicles and rat flexor digitorum longus (FDL) tendons represented positional and energy-storing tendons, respectively. The samples were stretched to incremental levels of strain, then stained with fluorescently labeled collagen hybridizing peptides (CHPs); the CHP fluorescence was measured to quantify denatured collagen. Denatured collagen in both positional and energy-storing tendons began to increase at the yield strain, upon leaving the linear region of the stress-strain curve as the sample started to permanently deform. Despite significant differences between the two tendon types, it appears that collagen denaturation is initiated at tissue yield during monotonic stretch, and the fundamental mechanism of failure is the same for the two types of tendons. At tissue failure, positional tendons had double the percentage of denatured collagen compared to energy-storing tendons, with no difference between 0% control groups. These results help to elucidate the etiology of subfailure injury and rupture in functionally distinct tendons.

Statement of significance

The collagen molecule is the fundamental structural unit in tendons, and becomes permanently denatured during mechanical overload. Therefore, understanding the onset and accumulation of denatured collagen in tendons relative to applied stretch is essential to understanding tendon failure. Furthermore, tendons are considered either positional or energy-storing depending on their physiological function. We previously showed that denatured collagen in positional tendons begins increasing at yield when the sample departs the linear region of the stress-strain curve and undergoes permanent deformation. This study demonstrates that the same is true for energy-storing tendons, and hence the fundamental mechanism of failure is preserved between both types of tendons. This has implications in common tendon injuries such as tendinopathy and acute rupture.

1. Introduction

Collagen is the major structural component of musculoskeletal tissues such as tendons, ligaments, and cartilage [1]. In a recent study, our lab demonstrated that permanent denaturation (damage, unfolding) of the collagen molecule occurs when rat tail tendon (RTT) fascicles are stretched via monotonic extension to sub-failure levels of strain [2]. It appeared that collagen denatu-

☆ Revised Article, Submitted, *Acta Biomaterialia* September 4, 2020
* Corresponding author at: Department of Biomedical Engineering, University of Utah, 50 South Central Campus Dr., Room 2480, Salt Lake City, UT 84112.
E-mail address: jeff.weiss@utah.edu (J.A. Weiss).

https://doi.org/10.1016/j.actbio.2020.09.056
1742-7061/

ration began to increase above baseline levels when the stress-strain curve departed the linear region and the tissue began to undergo permanent deformation. This was the first study to definitively show that a single event of sub-failure tissue level mechanical loading can directly cause collagen denaturation at the molecular level.

While this discovery was groundbreaking, it also raised questions about whether this observation would be consistent in the mechanical overload of other tendons under uniaxial extension. While tendons are defined as tissues that transfer load from muscle to bone, depending on their anatomical location and physiological function, there can be significant differences in biomechanics and biochemistry between different tendons [3–6]. Tendons are often classified as either 'positional' or 'energy-storing' [7]. These tendons have alternatively been referred to as 'weight bearing' or 'non-weight bearing' [8]. However, the tendons often used to compare these two tendon types (e.g. extensor and flexor tendons taken from the forelimbs of quadrupeds) can both bear weight, leading to ambiguity in the use of the latter terms. Therefore, we chose to use the former terminology because it describes the physiological function that these tendons ultimately perform. This terminology has also been widely used in the literature [3–5,9]. Positional tendons position joints, are described as 'cable' like, and include tail and extensor tendons. Energy-storing tendons store and release energy during motion, are described as 'spring' like, and include the Achilles, patellar, and flexor tendons [10]. The two tendon types also feature different collagen molecular crosslink profiles, with positional tendons having mostly divalent crosslinks, while energy-storing tendons have an increased density of trivalent crosslinks [3,4,9]. These differences led to the question of whether the failure mechanism of tendon and its effect on the collagen molecule differs between these two tendons types.

There is conflicting data regarding the location and mechanism of damage in tendons during uniaxial extension, and whether the mechanism(s) may differ between energy-storing and positional tendons. In studies on the effects of tension on sliding between microscale (fiber, fibril) structures, damage was defined as a permanent change in microstructure leading to changes in macroscale mechanical properties [8,11–13]. In both positional and energy-storing tendons (RTT fascicles and plantaris, respectively), damage was associated with non-recoverable interfibril and interfiber microscale sliding. This damage was correlated with a damage threshold at the inflection point on the stress-strain curve, defined as the point on the stress-strain curve at which strain-stiffening transitioned to strain-softening. While microscale sliding between the fibrils and fibers caused measurable damage in tissue level tensile tests, the microscale strain of these structures fully recovered following unloading in both tendon types, suggesting a lack of molecular level damage [8].

Other studies have focused on the collagen fibril level, identifying collagen damage in fibrils from scanning electron microscopy (SEM) images in the form of fibril kinking and changes in D-band spacing [4,14]. They are often supplemented by evidence such as increased susceptibility to trypsin digestion and changes in differential scanning calorimetry (DSC) curves, which are presented as evidence for collagen damage in the form of molecular level disruption [15,16]. Interestingly, this approach has demonstrated that molecular damage to collagen is dependent on both tissue type and strain-rate. Recently, Chambers et al. [9] stretched positional common digital extensor and energy-storing superficial digital flexor tendons to rupture at differing strain rates. They demonstrated that at a 'low' strain rate of 1%/s, there was significant molecular disruption following rupture in both tendon types. However, at a 'high' strain rate of 10%/s, energy-storing tendons lacked significant disruption of the collagen molecule. Therefore, there is evidence that energy-storing flexor tendons exhibit collagen denaturation at rupture, although the exact onset of this damage relative to the magnitude of applied strain is unknown.

Within the biomechanics community, there is a consensus that permanent tissue damage occurs when tendons are stretched to strain levels beyond the linear region of the stress-strain curve [2,17,18]. This transition, referred to as the yield point, occurs when the slope of the stress-strain curve begins to significantly decrease as the tissue softens [18]. In the study by Zitnay et al. [2], fluorescently labeled collagen hybridizing peptides (CHPs) were used to detect and measure molecular level collagen damage in tendons following monotonic stretch. Interestingly, the strain at the end of the linear region of the stress-strain curve (i.e. yield strain) appears to correspond with the strain at which CHP fluorescence (indicating denatured collagen) begins increasing [2]. This suggests that the yield strain could be the damage threshold for collagen denaturation during monotonic stretch in positional tendons. This is significant because denatured collagen is implicated in many injuries and diseases of musculoskeletal tissues in general (tendinopathy, osteoarthritis, cancer, etc.), and has been shown to be an essential part of collagen repair and homeostasis [2,19,20]. Since collagen is the major structural component of all tendons, and tissue softening indicates permanent tissue damage, we believe that collagen denaturation plays a major role in the failure of all tendons. Therefore, we hypothesized that both positional and energy-storing tendons would exhibit permanent collagen denaturation at the yield strain, despite their biomechanical and biochemical differences. The results of this study will help establish the onset of collagen denaturation relative to applied strain during monotonic stretch of different tendons types, helping us understand the etiology of injury and rupture in functionally distinct tendons.

2. Materials and methods

2.1. Sample collection and preparation

RTT fascicles and rat flexor digitorum longus (FDL) tendons were selected to represent positional and energy-storing tendons, respectively. The RTT fascicle is a positional tendon that has long served as a model tissue for studying tendon mechanics [18]. The FDL tendon is an energy-storing tendon [3,4,6,9,10] that has a high aspect ratio [21], making it ideal for tensile tests. Although it may seem that tissues from two different levels of the collagen hierarchy are being compared in this study, the tendons of small mammals such as rats and mice do not feature fascicles except in the special case of the rat tail tendon [22]. The RTT fascicles used in this case effectively function as a specialized positional tendon [22] and our description is consistent with the terminology that has been widely used in the literature [2,23,24]. Ultimately, both RTT fascicles and FDL tendons are one level above the fiber unit and on the size scale of millimeter, making them suitable for comparison. All tissue samples were from 12-16 week old male Sprague-Dawley rats. This age range was selected due to the biochemical profile of the collagen crosslinks at this age. The crosslinks are still predominantly enzymatic, as non-enzymatic advanced glycation end-products (AGEs) have not had an opportunity to accumulate due to age. Furthermore, the crosslinks in energy-storing tendons are primarily trivalent by this age [25]. While the divalent enzymatic crosslinks predominantly found in positional tendons may eventually develop into mature trivalent crosslinks, at 12-16 weeks of age, the crosslinks in RTT fascicles are still predominantly divalent [24,25].

RTT fascicles were dissected from rat tails (purchased from BioreclamationIVT, Westbury, NY) by twisting and pulling the distal end away, revealing fascicles. Rat FDL tendons were dissected from rat hind legs (purchased from BioreclamationIVT, Westbury,

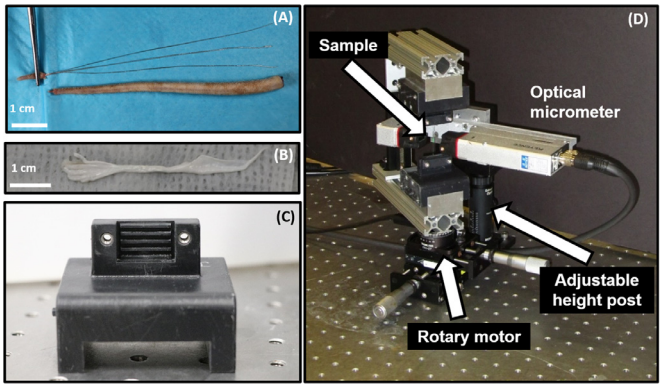

Fig. 1. Representative images of (A) RTT fascicles and (B) rat FDL tendon. (C) The samples were mounted in custom 3D printed clamps with trapezoidal ridges on the grip surface. This image shows one half of the custom clamp. (D) The cross-sectional area measurement rig. Samples are mounted in the rig and the rotary motor sweeps the sample 180°, while the cross-section is measured with the optical micrometer. Cross-sectional measurements are used to re-construct the cross-sectional geometry and determine the cross-sectional area for nominal stress calculations.

NY) by separating the tendon from the distal digits and isolating the FDL muscle. The muscle was rubbed away using gauze soaked in phosphate buffered saline (PBS). All samples were stored in PBS at -70 °C until they were mechanically tested.

The cross-sectional area of the samples was measured using a custom optical cross-sectional area measurement system (Fig. 1) prior to mechanical testing. Clamped samples were mounted vertically onto an adjustable height post and rotary motor. The height post was adjusted until there was no visible slack in the sample, and PBS was applied to the sample-clamp interfaces to permeate through the grips and help maintain total tissue hydration and ensure accurate cross-sectional area measurement. RTT fascicles were mounted in 3-D printed custom clamps. Five cross-sectional area measurements were made every 5 mm along the length of the sample. FDL tendons were mounted in 3-D printed custom clamps between sandpaper covered grips with cyanoacrylate. Due to the shorter initial length of the FDL tendons, only three cross-sectional area measurements were made along the length of the sample, spaced every 5 mm. Sample profile was measured as a function of angle of rotation using an optical micrometer (LS-9006M, Keyence Corporation, Osaka, Japan) through a 180° rotational sweep. Samples were rotated on a rotation stage (CR7-Z1, Thorlabs, Newton, NJ) at a rate of 1°/s, and measurements were acquired every 1 second. At each measurement acquisition, the sample profile was acquired at 16 kHz and averaged every 2048 samples. The resulting measurements of the profile widths were used to reconstruct the cross-sectional area using an algorithm by Langelier et al. [26] implemented in MATLAB (R2016b, Mathworks, Natick, MA), and the area calculated with the *polyarea* function. Measurements taken along the length of each sample were averaged to calculate a mean cross-sectional area for each sample. These values were used to construct the stress-strain curve for each sample.

2.2. Mechanical testing

Following cross-sectional area measurements, the sample, still mounted in the clamps, was transferred to a material test system (ElectroForce 3300 Series II, TA Instruments, Eden Prairie, MN). The sample was immersed in a PBS bath at room temperature throughout the duration of the test. A preload of 0.03 N was applied to the RTT fascicles, and the clamp-to-clamp distance was measured to establish the initial length, which defined 0% strain. A preload of 0.3 N was applied to FDL tendons, and the clamp-to-clamp distance measured for initial length, which defined 0% strain. The

Table 1
Material properties of RTT fascicles and rat FDL tendons when stretched at 0.5%/s. RTT fascicles were stiffer and stronger than FDL tendons; linear region modulus, UTS, and yield stress were greater in RTT fascicles, while cross sectional area, yield strain, and ultimate tensile strain were greater in FDL tendons. Mean ± S.E.M.

	Positional	Energy-storing	P-value
Cross sectional area (mm^2)	0.044 ± 0.004	1.30 ± 0.03	$p<0.0001$
Yield strain (%)	5 ± 2	17 ± 3	$p<0.0001$
Yield stress (MPa)	60 ± 20	21 ± 6	$p=0.0019$
Ultimate tensile strain (%)	7 ± 3	19 ± 3	$p=0.0002$
Ultimate tensile stress (MPa)	70 ± 20	25 ± 7	$p=0.0113$
Linear region modulus (MPa)	1,000 ± 400	180 ± 50	$p=0.0007$

preload level for RTT fascicles was based on our preliminary studies in advance of our previous publication that performed testing on RTT fascicles [2]. The preload level for the FDL tendons was chosen based on the relative difference in cross-sectional areas between the two tendon types (Table 1), in order to provide a similar starting stress for both tendon types. The mean ± SD gauge length was 36 ± 2 mm and 13 ± 1 mm for RTT fascicles and FDL tendons, respectively. Load data for RTT fascicles was collected at 2.5 kHz using a 5-lb load cell (WMC-5-460, Interface Inc., Scottsdale, AZ), while load data for FDL tendons was collected at 2.5 kHz using a 50-lb load cell (WMC-50-460, Interface Inc., Scottsdale, AZ). Sample preconditioning was not performed for either the RTT fascicles or FDL tendon. The mechanical testing protocol in this study followed the protocol used in our previous study, where preconditioning was also not performed [2]. Preconditioning damages the fascicle and reduces failure properties [27,28]. Since our study examined mechanical damage in tendons relative to applied strain, we wanted to remove those potential effects. Individual samples were monotonically loaded at 0.5%/s to a prescribed strain level. RTT fascicles were stretched to 0, 2.5, 3.75, 5, 6.25, 7.5, 9.25, 10, 11.25, 12.5, or 13.75% strain (n = 5 per strain level). FDL tendons were stretched to 0, 5, 10, 12.5, 15, 17.5, 20, 22.5, 25, 27.5, or 30% strain (n = 5 per strain level). These strain levels were selected based on the results of pilot studies to cover the full range of the stress-strain curve for both tissues while capturing the yield strain region. Power analysis was performed to determine the sample size required for CHP quantification based on pilot studies performed. Five samples per group were required to detect an effect size of 1.80, which represents the size of the difference between control tendons and tendons with increased amounts of denatured collagen. This was based on a two-tailed α (significance level) of 0.05 to provide a power (probability of not making a type II error) of 0.80. Following mechanical testing, the sample was unloaded and the clamped regions were trimmed away, isolating the tested region. All samples were stored in PBS at -70 °C until CHP staining.

2.3. Quantification of collagen denaturation

A CHP microplate assay was performed on all samples to measure the amount of denatured collagen via F-CHP fluorescence [29]. The samples were dabbed on lab cleaning tissue three times and their wet weight was recorded. Samples were then stained in 500 µL of 15 µM F-CHP (3Helix, Inc, Salt Lake City, UT) at 4 °C, overnight, with gentle agitation. After CHP staining, the samples were rinsed three times with 1 mL of PBS for 30 min at room temperature. The samples were then placed in 500 µL of a 1 mg/mL proteinase K (P2308, Sigma-Aldrich, St. Louis, MO) in deionized water solution at 60 °C for three hours to fully digest the tissue and release F-CHP into solution. The fluorescence of 200 µL duplicates of the digest was measured at excitation/emission wavelengths of 485/525 nm on a 96-well microplate reader (SpectraMax Gemini XPS, Molecular Devices, Sunnyvale, CA). These fluorescence

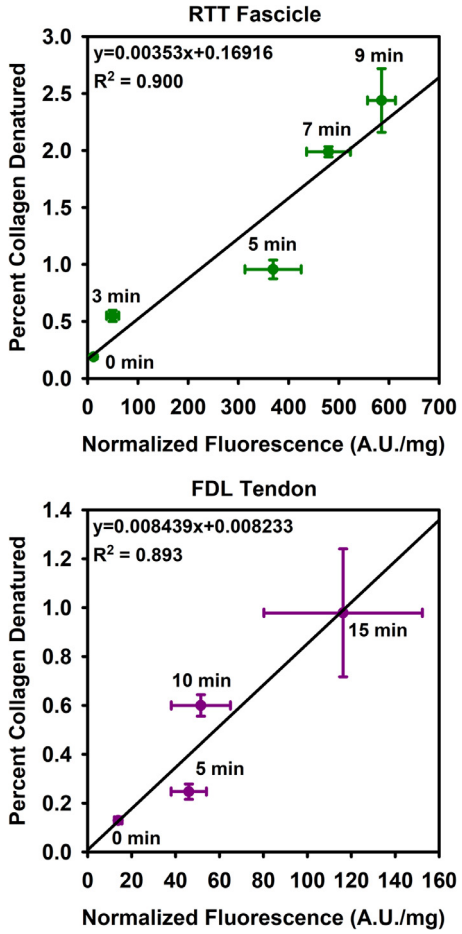

Fig. 2. Calibration curves correlating denatured collagen in terms of CHP fluorescence with percent of collagen denatured from trypsin digestion for RTT fascicles (top) and rat FDL tendons (bottom). Times indicate how long the samples were heated at 57 °C. Denatured collagen increased with heating time as measured by both the CHP microplate assay and the trypsin-hydroxyproline assay. Mean ± S.E.M.

values were averaged between duplicates and normalized to the wet weight of the tissue.

Separate calibration curves correlating the wet weight-normalized fluorescence with percent of collagen denatured were created for both tendon types using heat denatured tissue samples (Fig. 2). Different tendon types have different levels of water content, which affects the wet weight-normalized fluorescence values. Therefore, it was necessary to create independent calibration curves for both tendon types [30]. Our previous study demonstrated that these calibration curves accurately convert F-CHP fluorescence in mechanically damaged tendons to percent of collagen denatured, despite the calibration curve being created with thermally denatured samples [29]. Briefly, two sets of tissue samples for both tendon types were heat denatured at 57 °C for varying amounts of time. Temperature and heat times were determined in preliminary studies to ensure that the expected range of percent of collagen denatured in mechanically damaged tendons is captured by the calibration curves [23,29]. Two sets of RTT fascicles were heated for 0, 3, 5, 7, or 9 minutes (n = 5 per time, per set), while two sets of FDL tendons were heated for 0, 5, 10, or 15 min (n = 5 per time, per set). The amount of denatured collagen was quantified in one set using the CHP microplate assay, while the other set underwent the trypsin-hydroxyproline assay, as described in previous studies [19,29]. The results of both assays were correlated with each other to create the calibration curve for both tendon types. The trypsin-hydroxyproline assay calculates the amount of denatured collagen in terms of percentage of total collagen content [19], allowing the calibration curves for both respective tissues to convert the wet weight-normalized fluorescence values for all samples to percent of collagen denatured. The percent of collagen denatured was calculated for both tendon types at each strain level to compare the total amount of denatured collagen that accumulates during ramp to failure.

2.4. Data analysis

The cross-sectional area was used to construct a stress-strain curve for each sample. The average stress-strain curve was constructed for each strain level for both tendon types by calculating the mean stress at 0.001 strain intervals determined by linear interpolation [31]. We calculated the yield strain for each average stress-strain curve, which we defined as the strain where the tangent modulus had reduced to 50% of its maximum value [32]. The yield stress was defined as the stress at which the yield strain occurred. Linear region modulus was calculated as the slope of the linear region of the mean stress-strain curve for strain levels that reached a yield strain. We calculated the ultimate tensile strength (UTS) for each average stress-strain curve, which we defined as the point when the tangent modulus had reduced to zero; we calculated the stress and strain at this point.

2.5. Statistical analysis

The effect of strain level on the amount of denatured collagen was analyzed using one-way analysis of variance (ANOVA) followed by Dunnett's test for multiple comparisons, with the 0% strain groups serving as the control group for both tissue types. The percent of collagen denatured in the 0% controls and at the maximum strain level was compared between the two tendon types using a two-tailed *t*-test. We also compared the amount of denatured collagen in the strain group which correlated most closely to the calculated yield strain (5% and 17.5% for RTT fascicles and FDL tendons, respectively) with a two-tailed *t*-test. The cross-sectional area, yield strain, yield stress, strain at UTS, UTS, and linear region modulus were compared between the two tendon types using a two-tailed *t*-test. All statistical analyses were performed with SigmaPlot 13.0 (Systat Software, Inc., San Jose, CA, USA). Significance was set at $\alpha = 0.05$ for all statistical tests.

3. Results

3.1. Collagen denaturation between tendon types

The wet weight-normalized CHP fluorescence value for all samples was converted to percentage of collagen denatured using the calibration curves established for both tendon types (Fig. 2). Both calibration curves showed a linear relationship between the trypsin-hydroxyproline and CHP microplate assays for quantifying denatured collagen. The slope of the calibration curve for FDL tendons was greater than the slope for RTT fascicles, while the non-zero y-intercept was greater for RTT fascicles. The amount of denatured collagen in all samples was quantified and plotted relative to applied strain (Fig. 3). We defined an increase in the amount of denatured collagen as when the mean amount of denatured collagen at a certain strain level was more than 100% greater than the amount of denatured collagen at baseline (0% strain) (Table S1). In RTT fascicles, the amount of denatured collagen began increasing after 5% strain (Fig. 3, left). Strain groups 7.5% and greater had significantly different amounts of denatured collagen (p=0.023) than the 0% control group. The amount of denatured collagen measured in FDL tendons began increasing at 17.5% strain (Fig. 3, right),

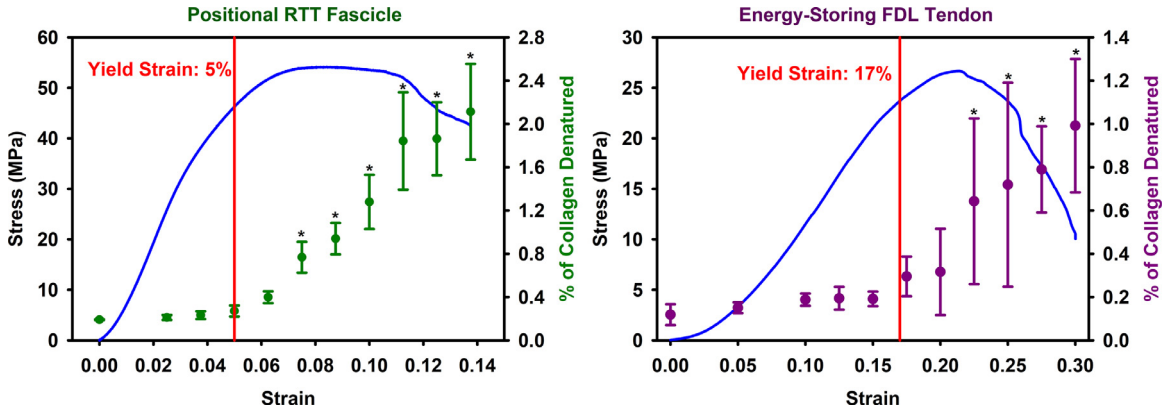

Fig. 3. Denatured collagen as measured by F-CHP fluorescence begins to increase at the yield strain in both tendon types. Mean stress strain curve to maximum strain in blue for RTT fascicles (left) and FDL tendons (right). Green and violet datasets are amounts of denatured collagen for RTT fascicles and FDL tendons, respectively. The red line indicates the yield strain for both tendons. Error bars represent 90% confidence intervals. $^{*}p < 0.05$ compared to 0% controls. (For interpretation of the references to color in this figure legend, the reader is referred to the web version of this article.)

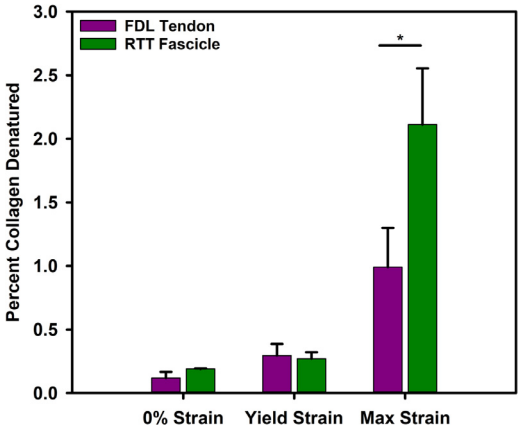

Fig. 4. The amount of denatured collagen was compared between the two tendon types at their respective yield strains and maximum strains. The amount of denatured collagen at baseline (0% strain) was also compared. RTT fascicles had significantly more denatured collagen than FDL tendons at the maximum strain level. The amount of denatured collagen was not significantly different between the two tendon types at baseline nor at their respective yield strains. Error bars represent 90% confidence intervals. $^{*}p < 0.05$ between tendon types.

with strain groups 22.5% and greater being significantly different ($p = 0.032$) than the 0% control group. The strain levels at which the denatured collagen began increasing were closely correlated with the yield strains: 5% and 17% for positional and energy-storing tendons, respectively. These results suggest that permanent collagen denaturation begins to accumulate upon the tissue yielding in both tendon types, despite differing biomechanical and biochemical properties.

The amount of denatured collagen was compared between the 0% controls, yield strain groups, and maximum strains groups, when the tissue had completely failed (Fig. 4). There was not a significant difference in the amount of denatured collagen between the 0% control RTT fascicles and FDL tendons. There was also not a significant difference in the amount of denatured collagen between RTT fascicles and FDL tendons which were stretched to their respective yield strains (5% and 17.5%, respectively). However, RTT fascicles exhibited a significantly greater amount of denatured collagen than FDL tendons at failure.

3.2. Effect of tendon type of biomechanical properties

RTT fascicles exhibited a greater UTS, yield stress, and linear region modulus compared to FDL tendons (Table 1). FDL tendons experienced greater strain at both the UTS and yield. The differences between the two tendon types for all values were found to be statistically significant. These results are consistent with previous reports that positional tendons are stiffer and stronger than energy-storing tendons [33].

4. Discussion

In both positional and energy-storing tendons, permanent collagen denaturation begins to accumulate once the tissue is stretched beyond the yield strain. This indicates that despite biomechanical and biochemical differences between the two tendon types, the fundamental molecular mechanism of failure appears to be the same. Previously, this link between yield strain and collagen damage accumulation had only been demonstrated by Zitnay et al. in positional tendons [2]. Up until the yield point, it is thought that individual collagen molecules within collagen fibrils engage in intermolecular sliding [9,34,35]. During this phase, the crosslinks resist excessive collagen intermolecular sliding and mediate load transfer between collagen molecules [2,9]. At the yield point, the crosslinks can no longer resist intermolecular sliding and α-chain sliding occurs [9,36,37]. Previously, we demonstrated through molecular dynamic simulations of microfibrils composed of collagen molecules that triple helix unfolding during tension likely occurs via α-chain sliding caused by shear-dominant loading [2]. This shear-dominant molecular unfolding mechanism disrupts the native triple helical structure and exposes binding site for CHPs [37]. As strain increases, the α-chains continue to slide out, further disrupting native triple helical structure, and exposing even more binding sites for CHP. This would explain why CHP fluorescence and denatured collagen accumulation occur after the yield strain. The yield strains for positional and energy-storing tendons were 5% and 17%, respectively, which closely correspond with the strain levels when denatured collagen begins to increase. However, the amount of denatured collagen was significantly different only for strain groups greater than 6.25% and 20%. This may be due to the yield point being calculated from the mean stress-strain curves for each strain group, and the variability in the yield strain between individual samples (Table 1). In reality, some samples within strain groups which were at or greater than the calculated yield strain did not reach the yield point, resulting in little or no denatured collagen and CHP fluorescence. Confirming this will require *in situ* monitoring of collagen denaturation during mechanical load.

As reported in Table 1, we observed a difference between the biomechanical properties of RTT fascicles and FDL tendons. One way to explain these differences is through the type and density of

intermolecular collagen crosslinks present in these tendon types. Energy-storing tendons have been shown to have higher valency and density of collagen crosslinks compared to positional tendons, which causes them to have greater resistance to inter-molecular sliding [9,36]. This results in a more 'brittle-like' behavior [36], which could explain why we observed a lower percentage of denatured collagen at tissue failure in FDL tendons compared to RTT fascicles. This is despite the two tendons types having the same amount of denatured collagen in 0% controls, meaning that healthy tendons of both types have the same amount of denatured collagen. Additionally, the lower valency and density of crosslinks found in positional tendons would allow the collagen fibrils to undergo plastic deformation more readily than energy-storing tendons. This is seen in the RTT fascicle stress-strain curve (Fig. 3, left) with the plateau region well past the yield point, but the FDL tendon stress-strain curve contains a more abrupt failure (Fig. 3, right). Malaspina et al. [38] performed simulations on the mechanical behavior of collagen fibrils, and the effect of crosslink removal. They found that decreasing crosslink density caused the shape of the stress-strain curves to transition from brittle to plastic failure, similar to the stress-strain curves for FDL tendons and RTT fascicles in this present study, respectively. The same study [38] performed simulated collagen fibril degradation, and found that a 3.3%wt volumetric degradation caused the stress-strain curve to lack a linear region, indicating an inability to bear load. While 3.3% represents a seemingly small amount, it is similar to results in our previous studies [2,29], in addition to the 2% calculated for RTT fascicles in this present study. Therefore, both experimental and computational experiments suggest that 2-3% denatured collagen is the upper bound of total collagen denaturation tendons are able to endure until failure.

The greater valency and density of crosslinks in energy-storing tendons may also resist permanent unfolding of the collagen molecule [3]. Chambers et al. demonstrated that both positional extensor and energy-storing flexor tendons exhibited significant molecular disruption when stretched to failure at 1%/s as evident by differences in DSC endotherms and changes observed in SEM images [9]. However, when stretched to failure at 10%/s, molecular disruption was only observed in positional tendons. This led to the description of plastic vs. brittle failure mode in tendons depending on tendon type and strain rate. In this study, all tensile testing was conducted at 0.5%/s, which corresponds with the plastic failure mode in both tendon types. Hence, the fact that we observed denatured collagen in energy-storing tendons stretched to failure is consistent with previous studies [9]. It would be interesting to perform a similar study at different strain rates to see if this brittle mode of failure has a corresponding difference in denatured collagen percentage and confirm these two modes of failure.

From a physiologic perspective, different crosslinks could reflect adaptations to the differing roles of these tendons [3,6,9,24]. In humans, a positional extensor tendon will experience significantly different loads and loading rates than an energy-storing Achilles tendon, which must withstand loads of full body weight for millions of cycles over the course of a lifetime. Different fiber microstructures highlight these differences, which also contribute to their differing biomechanical behavior (Table 1). For example, Lee et al. [12] found comparable micro-scale strain between RTT and plantaris tendons despite applying three times the tissue level strain to plantaris tendons; this suggests different degrees of interfibril and inter-fiber sliding during tissue level loading. Furthermore, energy-storing tendons can feature helical sub-structures, which help facilitate energy storage and return [5,39]. The consequence of these differences is seen in the differing biomechanical behavior of these tendons, especially in strain at yield and UTS. It would be interesting to examine the effect of these structural differences by comparing tissue level load to changes in fibril and molecular level strains using small angle X-ray scattering (SAXS) and wide angle scattering (WAXS), respectively [40]. Furthermore, SAXS could be used to examine changes in the ratio of the overlap region length relative to collagen fibril d-period lengths, which can be indicative of both collagen damage and cross-link density in the overlap regions [40].

The different properties between the two tendon types is also highlighted in the two distinct calibration curves (Fig. 2). Both calibration curves showed a linear relationship between the two methods of quantifying denatured collagen; however, they had different slopes and non-zero y-intercepts. These differences are likely due to distinct biochemical profiles between energy-storing and positional tendons, which affect their collagen thermal stability. Energy-storing tendons have superior thermal stability compared to positional tendons, which was shown to be likely due to greater crosslink density and valence [4]. This is also seen in our results, where energy-storing FDL tendons required greater heat denaturation times to create lower amounts of denatured collagen compared to positional RTT fascicles. The trypsin digestion method used to create the y-axis of the calibration curves is able to digest thermally unstable domains of triple-helical collagen which has not formed into fibrils, whereas CHPs only bind to uncoiled collagen molecules [41,42]. Therefore, while thermally unstable regions of the collagen molecules are digested by trypsin, they may not serve as a binding site for CHP. Greater thermal stability in energy-storing tendons compared to positional tendons would lead to lower CHP binding relative to comparable amounts of trypsin digestion. This would explain why wet weight normalized CHP fluorescence values for energy-storing FDL tendons were lower than positional RTT fascicles, which would lead to a greater slope for FDL tendons. Furthermore, energy-storing tendons have been shown to have lower rates of collagen turnover than positional tendons [43]. The thermally unstable domains would be more readily present in positional RTT fascicles due to greater collagen turnover rates, explaining the greater y-intercept for the RTT fascicle calibration curve. Regardless, our previous study showed that these calibration curves are able to accurately convert normalized fluorescence values to percent of collagen denatured [29].

One potential limitation of this study is the effect that the freeze-thaw cycle may have on the samples after they were mechanically damaged [44]. Samples were frozen immediately after trimming away the clamped regions, and all samples underwent the same protocol, so we expect minimal impact from the freeze-thaw cycle. Another potential limitation of this study is that tendon swelling due to PBS may affect the cross-sectional area measurements of the samples, leading to an underestimation of the stress values. Regardless, PBS is a standard buffer which is widely used during the mechanical testing of tendons.

Tendons endure millions of loading cycles during a person's lifetime; therefore, it is useful to consider the results of this study in the context of cyclic fatigue. Overuse injuries such as tendinopathy are thought to arise from 'micro-damage' accumulating over cycles. Our lab recently demonstrated that damage accumulation during the cyclic creep of positional RTT fascicles causes denaturation at the collagen molecule level [45]. Starting at a peak strain of approximately 4% (close to the yield strain calculated in the present study for RTT fascicles), the amount of denatured collagen above baseline was directly correlated with increasing peak strain. Additionally, the amount of denatured collagen at tissue failure following cyclic creep was similar to the amount measured in this study at RTT fascicle failure. This is additional evidence that collagen denaturation due to tissue-level load is a strain-mediated process. As for energy-storing tendons, very little data exists examining the amount of denatured collagen that accumulates during cyclic fatigue. Typically, energy-storing tendons are

thought to more readily resist fatigue damage than positional tendons in terms of resisting change to material properties [46,47]. Herod et al. [4] demonstrated that when positional and energy-storing tendons are loaded in cyclic creep, signs of collagen damage in the form of fibril kinking are seen in positional extensor tendons, but not energy-storing flexor tendons. However, the calculated peak strain was in the range of the yield strain for extensor tendons, while the peak strain for flexor tendons was far below its yield strain. Therefore, it is likely that no collagen molecular damage was observed in the flexor tendons because the tissue never reached its yield strain. Overuse injuries may only present themselves clinically when their cyclic loads exceed the yield strain and collagen molecular damage accumulation exceeds the rate of biological repair. This has been demonstrated in positional tendons; a topic of future study would be to confirm that this is the case with energy-storing tendons as well.

5. Conclusion

We have shown that permanent collagen denaturation begins to accumulate in measurable amounts once the yield strain has been reached in both positional and energy storing tendons. After this point, collagen denaturation continues to increase and accumulate with increasing strain in both positional RTT fascicles and energy-storing FDL tendons. Thus, the deformation mechanisms responsible for accumulation of collagen damage and subsequent failure at low strain rates are preserved across different tendons. Furthermore, the results of this study support evidence that collagen denaturation due to tissue-level loading is a strain-mediated process in tendons. Interestingly, the amount of denatured collagen measured in energy-storing tendons at tissue failure was half the amount found in positional tendons. This result, along with the differences in material properties between the two tendons types, can likely be explained by different enzymatic collagen crosslink profiles. The information presented here will aid scientists and clinicians in understanding how and why tendon injuries occur, especially in the context of tendon fatigue and overuse injuries, which will hopefully lead to improved treatment options and outcomes in the future.

Disclosures

S.M.Y. is a co-founder of 3Helix, Inc. which commercializes the collagen hybridizing peptides. All other authors have no professional or financial conflicts of interest to disclose.

Declaration of Competing Interest

S. Michael Yu is a co-founder of 3Helix, Inc. which commercializes the collagen hybridizing peptides. All other authors have no professional or financial conflicts of interest to disclose.

Acknowledgements

Financial support from NIH grants #R01AR071358 and R01EB015133 is gratefully acknowledged.

Supplementary materials

Supplementary material associated with this article can be found, in the online version, at doi:10.1016/j.actbio.2020.09.056.

References

[1] M.D. Shoulders, R.T. Raines, Collagen structure and stability, Annu. Rev. Biochem. 78 (2009) 929–958.
[2] J.L. Zitnay, Y. Li, Z. Qin, B.H. San, B. Depalle, S.P. Reese, M.J. Buehler, S.M. Yu, J.A. Weiss, Molecular level detection and localization of mechanical damage in collagen enabled by collagen hybridizing peptides, Nat. Commun. (2017) 8.
[3] A.S. Quigley, S. Bancelin, D. Deska-Gauthier, F. Legare, L. Kreplak, S.P. Veres, In tendons, differing physiological requirements lead to functionally distinct nanostructures, Sci. Rep. 8 (1) (2018) 4409.
[4] T.W. Herod, N.C. Chambers, S.P. Veres, Collagen fibrils in functionally distinct tendons have differing structural responses to tendon rupture and fatigue loading, Acta Biomater. 42 (2016) 296–307.
[5] C.T. Thorpe, C. Klemt, G.P. Riley, H.L. Birch, P.D. Clegg, H.R. Screen, Helical sub-structures in energy-storing tendons provide a possible mechanism for efficient energy storage and return, Acta Biomater. 9 (8) (2013) 7948–7956.
[6] R.E. Shadwick, Elastic energy storage in tendons: mechanical differences related to function and age, J. Appl. Physiol. 68 (3) (1990) 1033–1040 (1985).
[7] E.L. Batson, R.J. Paramour, T.J. Smith, H.L. Birch, J.C. Patterson-Kane, A.E. Goodship, Are the material properties and matrix composition of equine flexor and extensor tendons determined by their functions? Equine Vet. J. 35 (3) (2003) 314–318.
[8] A.H. Lee, D.M. Elliott, Multi-scale loading and damage mechanisms of plantaris and rat tail tendons, J. Orthop. Res. (2019).
[9] N.C. Chambers, T.W. Herod, S.P. Veres, Ultrastructure of tendon rupture depends on strain rate and tendon type, J. Orthop. Res. 36 (11) (2018) 2842–2850.
[10] H.R. Screen, S. Toorani, J.C. Shelton, Microstructural stress relaxation mechanics in functionally different tendons, Med. Eng. Phys. 35 (1) (2013) 96–102.
[11] S.E. Szczesny, D.M. Elliott, Interfibrillar shear stress is the loading mechanism of collagen fibrils in tendon, Acta Biomater. 10 (6) (2014) 2582–2590.
[12] A.H. Lee, S.E. Szczesny, M.H. Santare, D.M. Elliott, Investigating mechanisms of tendon damage by measuring multi-scale recovery following tensile loading, Acta Biomater. 57 (2017) 363–372.
[13] S. Duenwald-Kuehl, J. Kondratko, R.S. Lakes, R. Vanderby Jr., Damage mechanics of porcine flexor tendon: mechanical evaluation and modeling, Ann. Biomed. Eng. 40 (8) (2012) 1692–1707.
[14] S.P. Veres, J.M. Lee, Designed to fail: a novel mode of collagen fibril disruption and its relevance to tissue toughness, Biophys. J. 102 (12) (2012) 2876–2884.
[15] T.L. Willett, R.S. Labow, J.M. Lee, Mechanical overload decreases the thermal stability of collagen in an in vitro tensile overload tendon model, J. Orthop. Res. 26 (12) (2008) 1605–1610.
[16] S.P. Veres, J.M. Harrison, J.M. Lee, Mechanically overloading collagen fibrils uncoils collagen molecules, placing them in a stable, denatured state, Matrix Biol. 33 (2014) 54–59.
[17] P.P. Provenzano, K. Hayashi, D.N. Kunz, M.D. Markel, R. Vanderby Jr., Healing of subfailure ligament injury: comparison between immature and mature ligaments in a rat model, J. Orthop. Res. 20 (5) (2002) 975–983.
[18] B.J. Rigby, N. Hirai, J.D. Spikes, H. Eyring, The mechanical properties of rat tail tendon, J. Gen. Physiol. 43 (2) (1959) 265–283.
[19] R.A. Bank, M. Krikken, B. Beekman, R. Stoop, A. Maroudas, F.P. Lafeber, J.M. te Koppele, A simplified measurement of degraded collagen in tissues: application in healthy, fibrillated and osteoarthritic cartilage, Matrix Biol. 16 (5) (1997) 233–243.
[20] J.M. Weatherall, K. Mroczek, N. Tejwani, Acute achilles tendon ruptures, Orthopedics 33 (10) (2010) 758–764.
[21] D.T. Fung, V.M. Wang, D.M. Laudier, J.H. Shine, J. Basta-Pljakic, K.J. Jepsen, M.B. Schaffler, E.L. Flatow, Subrupture tendon fatigue damage, J. Orthop. Res. 27 (2) (2009) 264–273.
[22] A.H. Lee, D.M. Elliott, Comparative multi-scale hierarchical structure of the tail, plantaris, and Achilles tendons in the rat, J. Anat. 234 (2) (2019) 252–262.
[23] Y. Sun, W.L. Chen, S.J. Lin, S.H. Jee, Y.F. Chen, L.C. Lin, P.T. So, C.Y. Dong, Investigating mechanisms of collagen thermal denaturation by high resolution second-harmonic generation imaging, Biophys. J. 91 (7) (2006) 2620–2625.
[24] R.B. Svensson, S.T. Smith, P.J. Moyer, S.P. Magnusson, Effects of maturation and advanced glycation on tensile mechanics of collagen fibrils from rat tail and Achilles tendons, Acta Biomater. 70 (2018) 270–280.
[25] R.B. Svensson, H. Mulder, V. Kovanen, S.P. Magnusson, Fracture mechanics of collagen fibrils: influence of natural cross-links, Biophys. J. 104 (11) (2013) 2476–2484.
[26] E. Langelier, D. Dupuis, M. Guillot, F. Goulet, D. Rancourt, Cross-sectional profiles and volume reconstructions of soft tissues using laser beam measurements, J. Biomech. Eng. 126 (6) (2004) 796–802.
[27] R.C. Haut, The influence of specimen length on the tensile failure properties of tendon collagen, J. Biomech. 19 (11) (1986) 951–955.
[28] D.M. Elliott, P.S. Robinson, J.A. Gimbel, J.J. Sarver, J.A. Abboud, R.V. Iozzo, L.J. Soslowsky, Effect of altered matrix proteins on quasilinear viscoelastic properties in transgenic mouse tail tendons, Ann. Biomed. Eng. 31 (5) (2003) 599–605.
[29] A.H. Lin, J.L. Zitnay, Y. Li, S.M. Yu, J.A. Weiss, Microplate assay for denatured collagen using collagen hybridizing peptides, J. Orthop. Res. 37 (2) (2019) 431–438.
[30] H.L. Birch, Tendon matrix composition and turnover in relation to functional requirements, Int. J. Exp. Pathol. 88 (4) (2007) 241–248.
[31] C.M. Pollock, R.E. Shadwick, Relationship between body mass and biomechanical properties of limb tendons in adult mammals, Am. J. Physiol. 266 (3 Pt 2) (1994) R1016–R1021.
[32] A.G. Schwartz, J.H. Lipner, J.D. Pasteris, G.M. Genin, S. Thomopoulos, Muscle loading is necessary for the formation of a functional tendon enthesis, Bone 55 (1) (2013) 44–51.

[33] C.T. Thorpe, C.P. Udeze, H.L. Birch, P.D. Clegg, H.R. Screen, Specialization of tendon mechanical properties results from interfascicular differences, J. R. Soc. Interface 9 (76) (2012) 3108–3117.
[34] R. Puxkandl, I. Zizak, O. Paris, J. Keckes, W. Tesch, S. Bernstorff, P. Purslow, P. Fratzl, Viscoelastic properties of collagen: synchrotron radiation investigations and structural model, Philos. Trans. R. Soc. Lond. B Biol. Sci. 357 (1418) (2002) 191–197.
[35] N. Sasaki, S. Odajima, Elongation mechanism of collagen fibrils and force-strain relations of tendon at each level of structural hierarchy, J. Biomech. 29 (9) (1996) 1131–1136.
[36] B. Depalle, Z. Qin, S.J. Shefelbine, M.J. Buehler, Influence of cross-link structure, density and mechanical properties in the mesoscale deformation mechanisms of collagen fibrils, J. Mech. Behav. Biomed. Mater. 52 (2015) 1–13.
[37] S.G. Uzel, M.J. Buehler, Molecular structure, mechanical behavior and failure mechanism of the C-terminal cross-link domain in type I collagen, J. Mech. Behav. Biomed. Mater. 4 (2) (2011) 153–161.
[38] D.C. Malaspina, I. Szleifer, Y. Dhaher, Mechanical properties of a collagen fibril under simulated degradation, J. Mech. Behav. Biomed. Mater. 75 (2017) 549–557.
[39] T. Shearer, C.T. Thorpe, H.R.C. Screen, The relative compliance of energy-storing tendons may be due to the helical fibril arrangement of their fascicles, J. R. Soc. Interface 14 (133) (2017).
[40] F. Bianchi, F. Hofmann, A.J. Smith, M.S. Thompson, Probing multi-scale mechanical damage in connective tissues using X-ray diffraction, Acta Biomater. 45 (2016) 321–327.
[41] Y. Li, C.A. Foss, D.D. Summerfield, J.J. Doyle, C.M. Torok, H.C. Dietz, M.G. Pomper, S.M. Yu, Targeting collagen strands by photo-triggered triple-helix hybridization, Proc. Natl. Acad. Sci. U. S. A. 109 (37) (2012) 14767–14772.
[42] L. Ryhanen, E.J. Zaragoza, J. Uitto, Conformational stability of type I collagen triple helix: evidence for temporary and local relaxation of the protein conformation using a proteolytic probe, Arch. Biochem. Biophys. 223 (2) (1983) 562–571.
[43] H.L. Birch, S. Worboys, S. Eissa, B. Jackson, S. Strassburg, P.D. Clegg, Matrix metabolism rate differs in functionally distinct tendons, Matrix Biol. 27 (3) (2008) 182–189.
[44] C. Ding, M. Zhang, G. Li, Effect of cyclic freeze-thawing process on the structure and properties of collagen, Int. J. Biol. Macromol. 80 (2015) 317–323.
[45] G. S. J.L. Zitnay, G.S. Jung, A.H. Lin, Z Qin, Y Li, S.M. Yu, M.J. Buehler, J.A. Weiss, Accumulation of collagen molecular unfolding is the mechanism of cyclic fatigue damage and failure in collagenous tissues, Sci. Adv. 6 (35) (2020).
[46] J.H. Shepherd, K. Legerlotz, T. Demirci, C. Klemt, G.P. Riley, H.R. Screen, Functionally distinct tendon fascicles exhibit different creep and stress relaxation behaviour, Proc. Inst. Mech. Eng. H 228 (1) (2014) 49–59.
[47] C.T. Thorpe, G.P. Riley, H.L. Birch, P.D. Clegg, H.R.C. Screen, Fascicles and the interfascicular matrix show adaptation for fatigue resistance in energy storing tendons, Acta Biomater. 42 (2016) 308–315.